Majorana Fermions in Condensed Matter Physics: The 1D Nanowire Case

Philip Haupt, Hirsh Kamakari, Edward Thoeng, Aswin Vishnuradhan
Department of Physics and Astronomy, University of British Columbia, Vancouver, B.C., V6T 1Z1, Canada
(Dated: November 24, 2018)

Majorana fermions are fermions that are their own antiparticles. Although they remain elusive as elementary particles (how they were originally proposed), they have rapidly gained interest in condensed matter physics as emergent quasiparticles in certain systems like topological superconductors. In this article, we briefly review the necessary theory and discuss the "recipe" to create Majorana particles. We then consider existing experimental realisations and their methodologies.

I. MOTIVATION

Ettore Majorana, in 1937, postulated the existence of an elementary particle which is its own antiparticle, so called Majorana fermions [1]. It is predicted that the neutrinos are one such elementary particle, which is yet to be detected via extremely rare neutrino-less double beta-decay. The research on Majorana fermions in the past few years, however, have gained momentum in the completely different field of condensed matter physics. Artificially engineered low-dimensional nanostructures which show signatures characteristic of Majorana bound states have been shown to exist in the system of semiconductor nanowires [2–5], topological insulators [6], magnetic atom chains [7],etc., just to name a few. The outcome of these results shows that it is possible to simulate elementary particles using their quasiparticle counterpart in condensed matter systems.

Another big motivation for realizing Majorana fermions is the fact that they make ideal candidates for topological quantum computation circumventing the need for quantum error corrections and for minimizing the interactions with the environment . Quantum algorithms achieved via exchange of Majorana fermions (called 'braiding'), and qubit registers stored in spatially separated Majorana fermions are topologically protected from noise and decoherence. This means that small disturbances cannot decohere the qubit registers without inducing a topological phase transition. This unique advantage, combined with much lower error rates resulting from 'braiding' operations makes quantum computing with Majorana fermion networks the choice of companies such as Microsoft in the race to build the first universal quantum computer.

II. THEORY

A. Kitaev Toy Model

Although Majorana fermions were originally predicted in the context of elementary particle physics, they can also emerge in solid state systems as emergent quasiparticles as shown originally by Kitaev [8]. These are spin-$\frac{1}{2}$ particles which are their own antiparticles, and can be seen as a solution of the Dirac equation (see appendix A).

Kitaev used a simplified quantum wire model to show how Majorana modes might manifest as an emergent phenomena, which we will now discuss. Consider 1-dimensional tight binding chain with spinless fermions and p-orbital hopping. The use of unphysical spinless fermions calls into question the validity of the model, but, as has been subsequently realised, in the presence of strong spin orbit coupling it is possible for electrons to be approximated as spinless in the presence of spin-orbit coupling as well as a Zeeman field [9]. We require spinless fermions since we want to end up with single unpaired Majorana fermions (and so must get rid of all degeneracies, including spin degeneracy). We can write a non-interacting tight binding Hamiltonian with superconducting gap $\Delta = |\Delta| \exp(i\theta)$, hopping integral t, and chemical potential μ as

$$H = \sum_j [-\mu a_j^\dagger a_j - t(a_j^\dagger a_{j+1} + a_{j+1}^\dagger a_j) + \Delta a_j a_{j+1} + \Delta^* a_{j+1}^\dagger a_j^\dagger] \tag{1}$$

As usual, a_j and $a_j^\dagger$ denote annihilation and creation operators respectively.

We define the Majorana operators, with superconducting phase absorbed into their definitions, as

$$c_{2j-1} = \exp\left(i\frac{\theta}{2}\right) a_j + \exp\left(-i\frac{\theta}{2}\right) a_j^\dagger,$$
$$c_{2j} = -i\exp\left(i\frac{\theta}{2}\right) a_j + i\exp\left(-i\frac{\theta}{2}\right) a_j^\dagger,$$

for $j = 1, \ldots, N$ for an N atom chain. From the definition we immediately see that $c_i = c_i^\dagger$ for $i = 1, \ldots, 2N$ and therefore create particles which are their own antiparticles as required. It can also be shown that $\{c_i, c_j\} = 2\delta_{ij}$.

Let us now consider the case where $|\Delta| = t > 0$, $\mu = 0$. Here, equation (1) reduces to (using our new Majorana operators):

$$H = it \sum_{j=1}^{N-1} c_{2j} c_{2j+1}.$$

Now we can construct new creation and annihilation op-

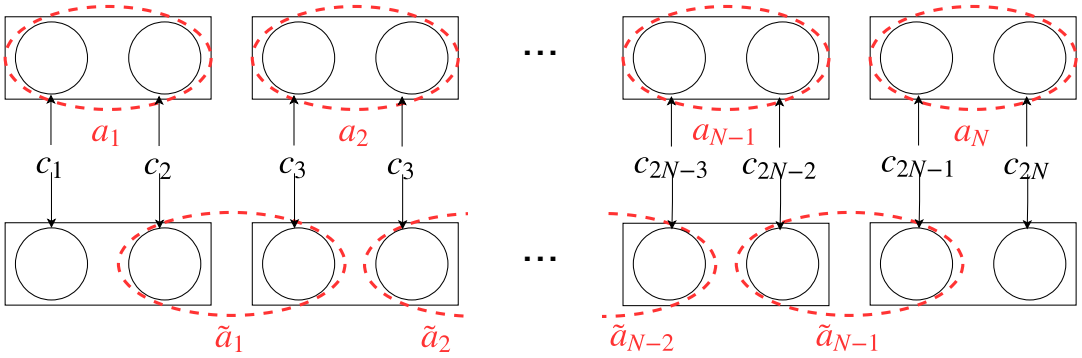

FIG. 1: Illustration for Kitaev's toy model, i.e. p-wave superconducting tight-binding chain. Each square represents an electron and the circles are Majorana fermions. Upper diagram: each Majorana operator c_{2i} and c_{2i-1} can be obtained by splitting fermion operator a_i. Lower diagram: case $|\Delta| = t > 0$, $\mu = 0$, the diagonalised Hamiltonian can be obtained by combining Majorana operators on neighbouring sites instead: this gives two unpaired operators c_1 and c_{2N}, which can be combined to give a non-local fermion operator $\tilde{a}_M$.

erators by combining Majorana operators on *neighbouring* sites.

$$\tilde{a}_j = \frac{1}{2}(c_{2j} + ic_{2j+1}),$$
$$\tilde{a}_j^\dagger = \frac{1}{2}(c_{2j} - ic_{2j+1}).$$

The Hamiltonian from equation (1) now becomes

$$H = 2t\sum_{j=1}^{N-1}\left(\tilde{a}_j^\dagger\tilde{a}_j - \frac{1}{2}\right).$$

For an illustration of the discussion so far, see FIG. 1.

Here we can see that the $\tilde{a}_j$ operators correspond to Fock . Notice, however, that the Majorana operators c_1 and c_{2N} are completely absent from this diagonalised Hamiltonian. These can be combined to a single, highly non-local fermionic operator

$$\tilde{a}_M = \frac{1}{2}(c_1 + c_{2N})$$

Occupying this state requires zero energy (since it does not appear in the Hamiltonian), and thus we can have an odd number of quasiparticles at zero energy cost (unlike the superconductors we are used to, where we require an even number, i.e. Cooper pair condensates). This evenness/oddness is called parity and can be determined by the eigenvalue of $\tilde{a}_M^\dagger\tilde{a}_M$ (0 for even or 1 for odd parity).

Although we only showed this for a special case, namely $|\Delta| = t > 0$, $\mu = 0$, Kitaev showed that the Majorana edge states (called Majorana zero modes, MZMs) exist as long as $|\mu| < 2t$ [8] (i.e. μ is inside the gap). More generally, these Majorana states may not be localised, but instead decay exponentially away from the ends.

B. Mapping Kitaev Model in Semiconductors

Kitaev's toy-model's key ingredient is spinless nearest neighbour p-wave superconductivity which has not been realised in real materials. In 2010, however, two seminal papers show how to map the Kitaev p-wave quantum wire to an s-wave quantum wire in the presence of strong spin orbit coupling and a magnetic field. [10, 11]. The resulting Hamiltonian, without superconductivity, is

$$H = \sum_{k,k',\sigma,\sigma'} H_{k,k',\sigma,\sigma'}a_{k\sigma}^\dagger a_{k'\sigma'},$$
$$H_{k,k',\sigma,\sigma'} = \langle k\sigma|\frac{\boldsymbol{p}^2}{2m} - \mu + \alpha\hat{\boldsymbol{n}}\cdot(\boldsymbol{\sigma}\times\boldsymbol{p}) + B\sigma_z|k'\sigma'\rangle.$$

Here the magnetic field is aligned along the wire (in the positive z direction), $\hat{\boldsymbol{n}}$ is perpendicular to the plane in which the wire lies, and $\boldsymbol{\sigma}$ is the vector of Pauli matrices. In our case the term $\hat{\boldsymbol{n}}\cdot(\boldsymbol{\sigma}\times\boldsymbol{p})$ simplifies to $\sigma_x p_z$. This Hamiltonian is simply diagonlized, with the resulting energy spectrum being

$$E(k_z) = \frac{\hbar^2k_z^2}{2m} - \mu \pm \sqrt{\alpha^2k_z^2 + B^2}.$$

If we now introduce BCS superconductivity with the gap parameter Δ, the new Hamiltonian can be diagonalized using the Bogoliubov-de-Gennes transformation [12], resulting in the new dispersion relation

$$E^2(k_z)_\pm = \left(\frac{\hbar^2k_z^2}{2m} - \mu\right)^2 + (\alpha k_z)^2 + B^2 + \Delta^2$$
$$\pm 2\sqrt{(B\Delta)^2 + [B^2 + (\alpha k_z)^2]\left(\frac{\hbar^2k_z^2}{2m} - \mu\right)^2}.$$

The effects of the different components of the Hamiltonian is shown in FIG. 2 as a function of increased magnetic field. Magnetic field induces topological transitioni

which ends (in the figure) with the topological superconducting bulk state with Majorana fermions at the edge of the nanowire.

III. EXPERIMENTAL REALIZATION

A. Material Choice and Device Fabrication

As shown in the previous section, Majorana Zero Modes (MZMs) can be obtained by tuning chemical potential or magnetic field to drive the system towards topological superconductor phase. The other components of the 'recipe' (spin-orbit coupling, proximitized superconductivity) are intrinsic material properties. The common choice for the 1D nanowire with strong spin-orbit interaction so far has been the heavy element semiconductors InSb and InAs[10]. The two criteria, superconductivity and magnetic field, compete in a way that large magnetic field can destroy the triplet pairing in the induced superconductivity. A large Zeeman splitting, however, is required in order to prevent interaction between the pairs of Majorana fermions (at the same edge location) of the two spin channels, which combines into fermionic mode at zero energy. Therefore, nanowire with a large Lande g-factor is desired to obtain large Zeeman splitting at fields below the critical field of s-wave superconductor.

The choice of superconductors, correspondingly, require a large superconducting gap and high critical field to withstand the applied in-plane magnetic fields. In the experiments so far, two different superconductors have been used: NbTiN (Type-II superconductor) and Al (Type-I). The first generation of the device used NbTiN due to its much higher critical field. It was discovered, however, that Al has two main advantages in terms of higher interface quality and a type-I hard superconducting bandgap as compared to NbTiN. Higher interface results from capability of in-situ deposition of Al, which suppress undesired sub bandgap density of states. Al as type-I superconductor has an additional benefit of not having issues with vortices disturbances created by magnetic field in type-II superconductor. This vortices are suspected to turn the band gap into a 'soft gap' which degrades the conductance signal of MZMs[5, 10]. The device schematics of the first and latest generation of MZMs nanowire are shown in fig. 4.

B. Signature of Majorana Fermions: Zero Bias Peak

Low-bias transport of a normal metal-superconductor interface is predominantly determined by the Andreev reflection, in which incident electron is reflected as a hole and a Cooper pair is created in the superconductor resulting in a net charge transfer of $2e$. Differential conductance is related to the probability of electron reflected as a hole ($|r_{eh|^2}$) by:

$$G(V) = \frac{dI}{dV} = 2G_0|r_{eh}|^2, \tag{2}$$

where $G_0 = \frac{e^2}{h}$ is the conductance quanta. If a zero energy mode is present in the superconductor, the reflection amplitude is maximized $|r_{eh}|^2 = 1$ similar to the resonant tunneling from equal double barriers which results to perfect Andreev reflection and $G = 2G_0$. Resonant tunneling measurement provides the local density of states of this interface where the MZMs are expected to reside.

The InAs/Al device tunneling schematic is shown in lower part of fig.4, and the differential conductance results are shown in fig. 6. The conductance spectrum shows the topological transition from trivial superconductor (the normal proximited superconductivity) into the topological superconductivity with MZMs at critical magnetic field, $B_c = \sqrt{\Delta^2 + \mu^2} \approx 0.7$ Tesla. Zero bias peak (ZBP) is not unique to MZMs, but further investigations have eliminated the false positives coming from e.g. local Andreev bound states, disorder-induced zero-bias states, etc. Furthermore, the measured ZBP was shown not to depend on the tunneling barrier height as in the case of local Andreev bound states and is the characteristic of robust topological MZMs[5, 10].

IV. FUTURE DIRECTIONS: TOWARDS QUANTUM COMPUTING WITH MAJORANA FERMIONS

The results published in [5] shows a very convincing evidence of the Majorana bound states (MZMs) in the semiconductor nanowire devices. The next step would be to prove the possibility of creating a nanowire junction and readout for 'braiding' operation. As mentioned in the introduction, quantum computing operation is obtained via exchaging the adjacent Majorana fermions and this operations forms a 'weave' pattern unique to that particular operation. In 1D nanowire, however, there is only one channel for the Majorana fermion to move around. Therefore, a junction is required to allow one Majorana to exit the channel, before switching its location to the neighboring Majorana fermions (fig. 7. By forming 'trenches' on the substrate, network of nanowire can be grown from the bottom-up to form what is called a 'hashtag' circuit (fig.8). Preliminary measurements of this 'hashtag' have shown phase coherent transport, and therefore shows a very promising development for real-world topological quantum computing in the near future.

V. CONCLUSION

This short report was intended to give a brief overview of the physics of Majorana fermions, an ever-growing subject of interest, especially in condensed matter physics.

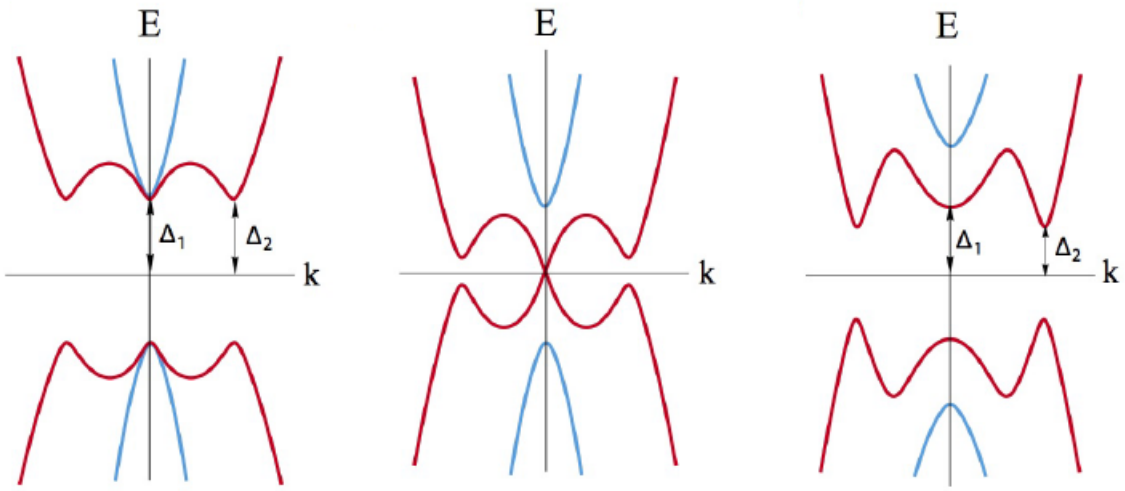

FIG. 2: Semiconductor nanowire proximitized with s-wave superconductivity as magnetic field is increased. Left:Trivial (normal s-wave) superconducting phase. Middle: Crossing of energy band occur as a result of topological transition with delocalized Majorana across nanowire. Right: Re-opening of the gap into the topological superconducting state with localized Majorana at the edges of nanowire (Majorana Zero Modes). Δ_1 and Δ_2 are superconducting gap at $k = 0$ and k_F which magnitude differ in the topological superconducting phase.[13]

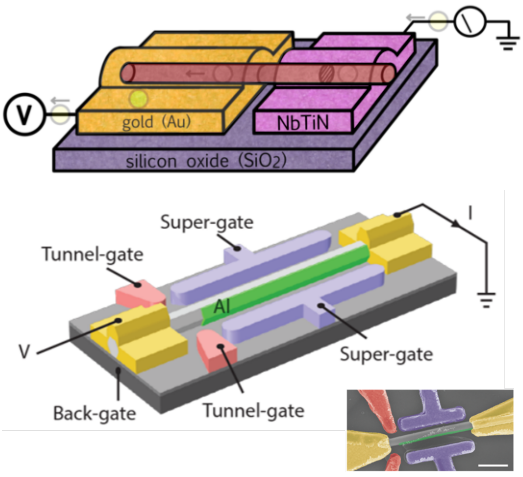

FIG. 4: Upper: First generation of InSb/NbTiN nanowire MZMs device[14]; Lower: Latest generation of InSb/Al schematics (inset shows false-color electron micrograph)[10].

We illustrated the fundamental principles in a simplified toy model, first proposed by Kitaev, then discussed one of the first experimental realisations and the methodologies used to find Majorana fermions by mapping Kitaev p-wave superconductivity to semiconductor nanowires. The devices and signatures resulting from Majorana Zero Modes (MZMs) have been shown which shows a strong indication of localized Majorana fermions in the nanowire edges. This is the unique feature of the topological superconducting phase. Furthermore, the current status of realizing a scalable quantum computer using nanowires is being pursued, showing very promising results for a more robust and fault tolerant topological quantum computer using Majorana Fermions.

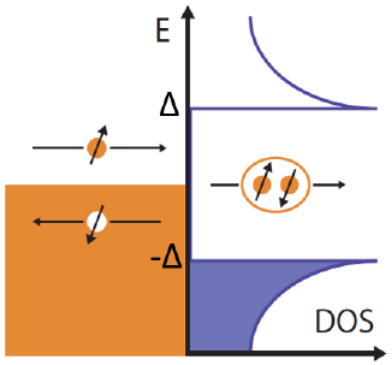

FIG. 5: Andreev resonant tunneling in metal/superconductor interface in the presence of MZMs or zero energy bound states[10].

[1] E. Majorana, Il Nuovo Cimento (1924-1942) **14**, 171 (2008), ISSN 1827-6121, URL `https://doi.org/10.1007/BF02961314`.

[2] V. Mourik, K. Zuo, S. M. Frolov, S. R. Plissard, E. P.

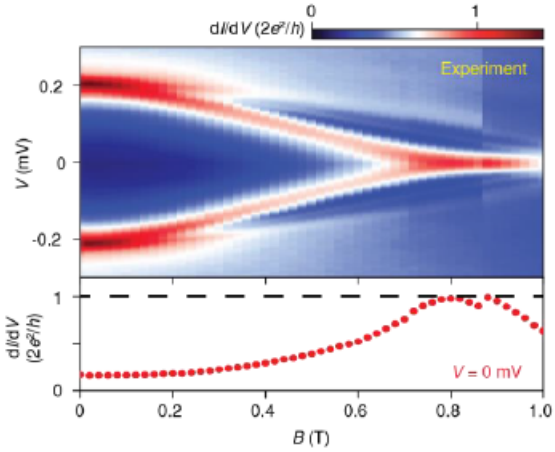

FIG. 6: Upper:Tunneling conductance as a function of in-plane magnetic field. Lower: Horizontal slice of the zero-bias peak which shows quantized conductance ($2G_0$) on the onset of MZMs transition ($\approx$ 0.7 Tesla). The measurement temperature is at T=20 mK.[5]

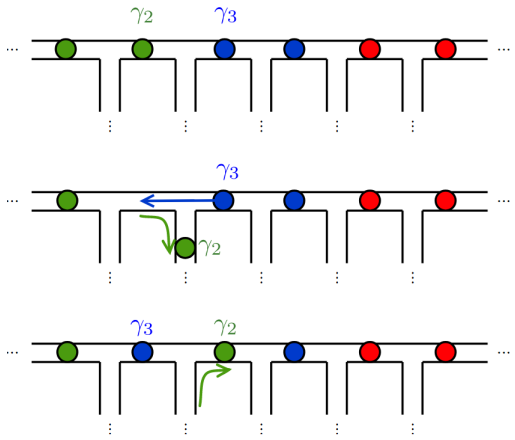

FIG. 7: Switching Majorana operation in 1D nanowire requires an exit junction. Shown here is the simplest 'T-junction'[15].

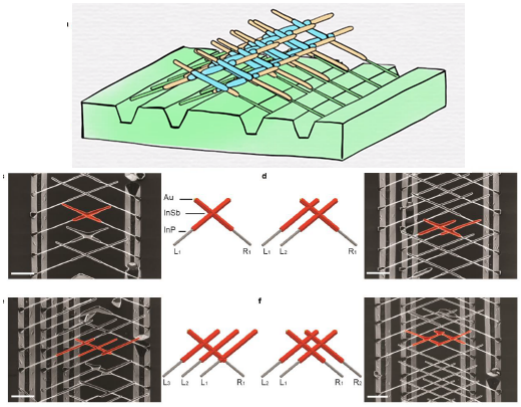

FIG. 8: Nano-'hashtag' network built with semiconductor nanowires for future topological quantum computing device (modified from [16, 17]).

A. M. Bakkers, and L. P. Kouwenhoven, Science **336**, 1003 (2012), ISSN 0036-8075.

[3] H. Zhang, . Gl, S. Conesa-Boj, M. P. Nowak, M. Wimmer, K. Zuo, V. Mourik, F. K. de Vries, J. van Veen, M. W. A. de Moor, et al., Nature Communications **8**, 16025 (2017), URL `https://doi.org/10.1038/ncomms16025`.

[4] . Gl, H. Zhang, J. D. S. Bommer, M. W. A. de Moor, D. Car, S. R. Plissard, E. P. A. M. Bakkers, A. Geresdi, K. Watanabe, T. Taniguchi, et al., Nature Nanotechnology **13**, 192 (2018), ISSN 1748-3395, URL `https://doi.org/10.1038/s41565-017-0032-8`.

[5] H. Zhang, C.-X. Liu, S. Gazibegovic, D. Xu, J. A. Logan, G. Wang, N. van Loo, J. D. S. Bommer, M. W. A. de Moor, D. Car, et al., Nature **556**, 74 (2018), URL `https://doi.org/10.1038/nature26142`.

[6] Q. L. He, L. Pan, A. L. Stern, E. C. Burks, X. Che, G. Yin, J. Wang, B. Lian, Q. Zhou, E. S. Choi, et al., Science **357**, 294 (2017), ISSN 0036-8075.

[7] S. Nadj-Perge, I. K. Drozdov, J. Li, H. Chen, S. Jeon, J. Seo, A. H. MacDonald, B. A. Bernevig, and A. Yazdani, Science **346**, 602 (2014), ISSN 0036-8075.

[8] A. Y. Kitaev, Physics-Uspekhi **44**, 131 (2001), URL `http://stacks.iop.org/1063-7869/44/i=10S/a=S29`.

[9] S. R. Elliott and M. Franz, Rev. Mod. Phys. **87**, 137 (2015), URL `https://link.aps.org/doi/10.1103/RevModPhys.87.137`.

[10] R. M. Lutchyn, E. P. A. M. Bakkers, L. P. Kouwenhoven, P. Krogstrup, C. M. Marcus, and Y. Oreg, Nature Reviews Materials **3**, 52 (2018), ISSN 2058-8437, URL `https://doi.org/10.1038/s41578-018-0003-1`.

[11] Y. Oreg, G. Refael, and F. von Oppen, Phys. Rev. Lett. **105**, 177002 (2010), URL `https://link.aps.org/doi/10.1103/PhysRevLett.105.177002`.

[12] J. Cayao, ArXiv e-prints (2017), 1703.07630.

[13] R. Aguado (2017), arXiv:1711.00011.

[14] QuTech Delft, *img-ballistic-transport*, [Online; accessed November 23, 2018], URL `https://qutech.nl/external/timeline/afbeeldingen/img-ballistic-transport.png`.

[15] QuTech, *nanowire network exchange*, [Online; accessed November 23, 2018], URL `https://topocondmat.org/w2_majorana/figures/nanowire_network_exchange.svg`.

[16] TU Eindhoven, *Nano-hashtags could provide definite proof of majorana particles* (2017), [Online; accessed November 23, 2018], URL `https://www.youtube.com/watch?v=aakSpSXLSYY`.

[17] S. Gazibegovic, D. Car, H. Zhang, S. C. Balk, J. A. Logan, M. W. A. de Moor, M. C. Cassidy, R. Schmits, D. Xu, G. Wang, et al., Nature **548**, 434 (2017), URL `https://doi.org/10.1038/nature23468`.

[18] R. Shankar, *Principles of quantum mechanics* (Plenum Press, 1994), 2nd ed., ISBN 978-0-306-44790-7.

[19] M. E. Peskin and D. V. Schroeder, *An introduction to quantum field theory*, Frontiers in Physics (Perseus Books Publishing, L.L.C., 1995), ISBN 0201503972,9780201503975.

Appendix A: Majorana's Solution to the Dirac Equation

The relativistic Dirac equation can be derived [18] by replacing the classical Hamiltonian $\frac{\hat{\boldsymbol{p}}^2}{2m} + V(\hat{x}, t)$ in the Schrödinger Equation with the relativistic Hamiltonian $\sqrt{\boldsymbol{p}^2 + m^2}$, in which case the corresponding equation of motion becomes

$$i\frac{\partial}{\partial t}\psi = \sqrt{\boldsymbol{p}^2 + m^2}\psi.$$

To obtain a Lorentz invariant form of the equation, we can rewrite $\boldsymbol{p}^2 + m^2$ as the square of a different quantity, $\boldsymbol{p}^2 + m^2 = (\boldsymbol{\alpha}\cdot\boldsymbol{p} + \alpha_0 m)^2$ for some objects $\boldsymbol{\alpha} = (\alpha_1, \alpha_2, \alpha_3)$ and α_0. Upon squaring the quantity $\boldsymbol{\alpha}\cdot\boldsymbol{p} + \beta m$ and equating with $\boldsymbol{p}^2 + m^2$, we obtain the relations

$$\begin{cases} \alpha_i^2 = 1 \\ \{\alpha_i, \alpha_j\} = 0 \end{cases},$$

which can be satisfied by setting

$$\boldsymbol{\alpha} = \begin{pmatrix} 0 & \boldsymbol{\sigma} \\ \boldsymbol{\sigma} & 0 \end{pmatrix}, \qquad \alpha_0 = \begin{pmatrix} I & 0 \\ 0 & -I \end{pmatrix}.$$

The resulting Dirac equation is $i\frac{\partial}{\partial t}\psi = (\boldsymbol{\alpha}\cdot\hat{\boldsymbol{p}} + \alpha_0 m)\psi$. Since the α_i's are 4×4 matrices, the solutions ψ must be 4 component spinors. In the case of charged spin-$\frac{1}{2}$ particles, which the Dirac equation was initially derived to describe, the components correspond to the two spin states of the electron and the two spin states of the positron. In the Weyl representation, with

$$\gamma^0 = \begin{pmatrix} 0 & 1 \\ 1 & 0 \end{pmatrix}, \qquad \gamma^i = \begin{pmatrix} 0 & \sigma^i \\ -\sigma^i & 0 \end{pmatrix},$$

the equation can be rewritten as $(i\gamma^\mu\partial_\mu - m)\psi = 0$ [19].

The choice of matrices γ^μ are not unique. In particular, as realised originally by Majorana in 1937, if the γ matrices are chosen as

$$\gamma^0 = i\begin{pmatrix} 0 & -\sigma^1 \\ \sigma^1 & 0 \end{pmatrix}, \ \gamma^1 = i\begin{pmatrix} 0 & \sigma^0 \\ \sigma^0 & 0 \end{pmatrix}$$

$$\gamma^2 = i\begin{pmatrix} \sigma^0 & 0 \\ 0 & -\sigma^0 \end{pmatrix}, \ \gamma^3 = \begin{pmatrix} 0 & \sigma^2 \\ -\sigma^2 & 0 \end{pmatrix}$$

the solutions to the Dirac equation in this are real valued and neutral. The spinor ψ now describes a spin-$\frac{1}{2}$ particle which is its own antiparticle, a Majorana fermion [9].